A better understanding of continuous welded rail track

Prof.Dr.Ir. Coenraad Esveld
Professor of Railway Engineering at TU Delft & Consultant to ERRI

In 1992, the International Union of Railways (UIC) commissioned a study from the European Rail Research Institute (ERRI) entitled 'Improved knowledge of CWR, including switches'. The work was assigned to the ERRI D 202 Specialists' Committee. There are basically four parts to the work:

— development of theoretical models;
— experimental work to determine input values for the models and to validate the models;
— revision of UIC leaflets on continuous welded rail (CWR);
— non-destructive measurement of longitudinal rail forces due to temperature.

Most of the basic work on the models has now been completed. Three models have been developed at the TU Delft, The Netherlands, and the TU Kraków, Poland, namely:

— CWERRI, which analyses CWR track stability in combination with longitudinal and vertical loads, including dynamic effects and yielding of ballast under combined load situations;
— CREEP, which permits analysis of creep phenomena under longitudinal train loads and also modelling of curve breathing;
— TURN, a finite element model that allows analysis of turnouts and generates super elements for use in CWERRI.

In the following paragraphs a description is given of these three models and the results available discussed [1].

CWERRI – CWR track analysis

ERRI assigned the task of developing CWERRI to the TU Delft. The program allows the longitudinal, vertical and lateral behaviour of CWR track to be modelled and calculated integrally in a user-friendly environment. The basic features of the model are as follows:

— three-dimensional modelling and calculation;
— longitudinal, lateral and vertical forces;
— lateral and vertical track stability;
— thermal and mechanical loads;
— complete train loads, taking uplift waves into account;
— three-dimensional ballast yield, taking the influence of vertical loads into account;
— track/bridge interaction, including the effects of bridge-end rotation;
— multi-span bridges with parallel tracks.

Buckling analysis of curved CWR track

Using the CWERRI model, a sensitivity analysis was carried out on the track structure represented in Fig. 1, by varying such parameters as the half wavelength of the misalignment, the curve radius, the peak and limit resistance of the lateral ballast strength and the torsional stiffness of the fastening system [2]. The dimensions and properties were chosen in accordance with results published in [3]. The track model was 47.5 m long, with a horizontal curve radius of 400 m. A longitudinal spring was added at the boundaries, in order to model the longitudinal behaviour of linear elastic tangent track up to infinity. The misalignment in the middle was characterised by a half sine wave with a length of 9.144 m (360 in.) and an amplitude of 0.0381 m (1.5 in.). The track component properties were as follows:

— rails: AREA#136;
— sleeper spacing: 0.61 m;
— vertical ballast stiffness: 68,900 kN/m per metre of track.

The constitutive behaviour of the ballast spring is given in Fig. 2. The values for F_p and F_l in the absence of vehicle load are given in the following table.

Parameter		Fixed value	Range
Radius	[m]	400	100-tangent
Lateral peak resistance (F_p)	[N per m track]	17508	8754-26262
Lateral limit resistance (F_l)	[N per m track]	9630	4815-14445
Longitudinal stiffness	[N/m per m track]	1.378e6	1.0e5-1.0e7
Torsional stiffness	[Nm/rad per m track]	1.1125e5	0.0-3.0e5
Amplitude of misalignment	[m]	0.0381	0.008-0.05
Half wavelength of misalignment	[m]	4.572	1.2-9.6

Parameters used in buckling sensitivity study

The track was loaded vertically by a hopper wagon with two bogies, represented by four vertical axle loads of 293 kN each, as indicated in Fig. 3.

The track was loaded by increasing the temperature from 0°C to 100°C. Fig. 4 shows lateral deformation in the centre of the model against temperature increase. In [2] these results were compared with the values produced by the model described in [3], which was validated by a number of full-scale track buckling tests carried out in the USA, both with and without moving trains. The values produced by both models are very close. The plot represented in Fig. 4 is characterised by two points. The first point is the temperature T_{max} (49.4°C), the highest point in the figure, at which buckling starts. After this point, the temperature drops and deformations increase rapidly. The second point is the minimum temperature T_{min} (33.5°C) which occurs after buckling has started. From a safety point of view this is the most important value.

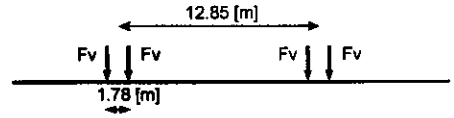

Fig. 3: Vertical load applied on track model (F_v = 293 kN)

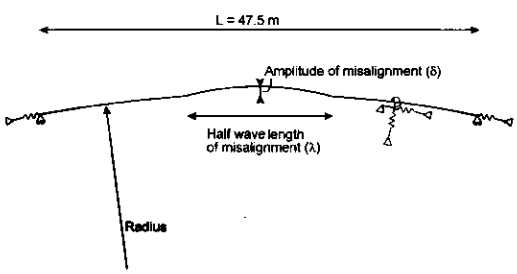

Fig. 1: Top view of track model studied

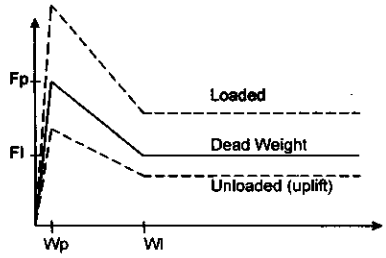

Fig. 2: Model of lateral ballast behaviour for different vertical loadings

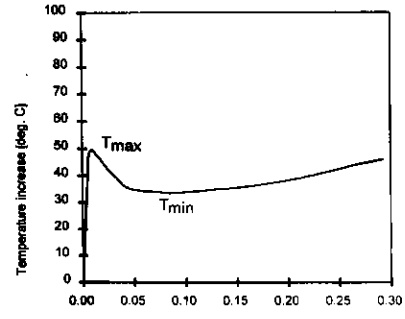

Fig. 4: Lateral deformation at the centre of the model

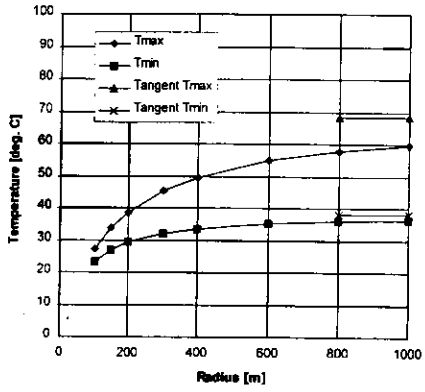

Fig. 5: Influence of radius

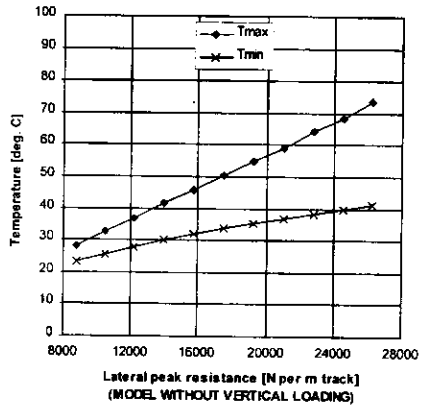

Fig. 6: Influence of lateral peak resistance

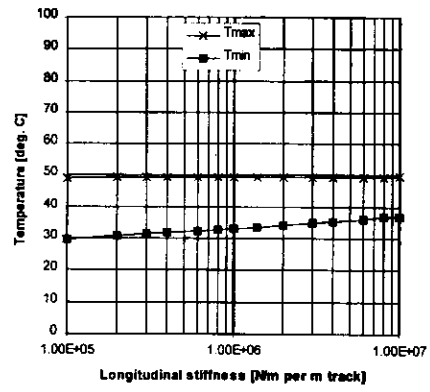

Fig. 7: Influence of longitudinal stiffness

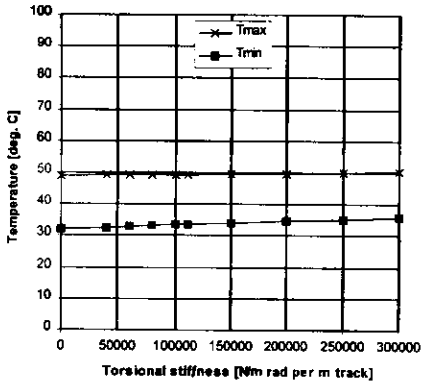

Fig. 8: Influence of torsional stiffness

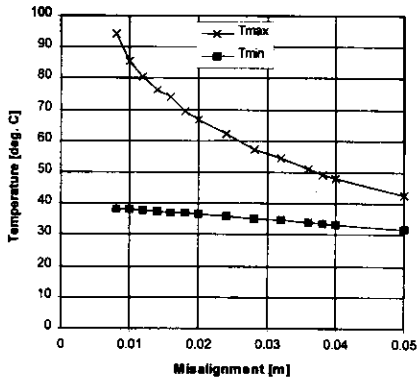

Fig. 9: Influence of misalignment

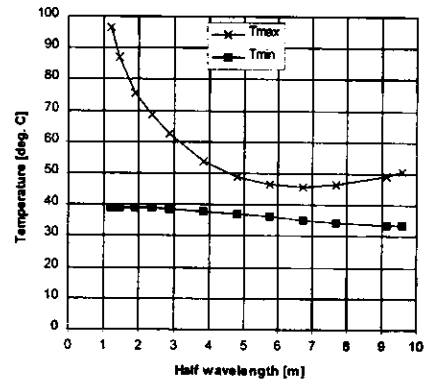

Fig. 10: Influence of half wavelength

Sensitivity analysis: this concerns the sensitivity of T_{max} and T_{min} to the parameter variations shown in the table. Each parameter was varied over a practical range while keeping all other parameters constant at the 'fixed value' shown in the table. The ballast yield force is affected by the vertical track load. In the sensitivity results presented here this effect has not been taken into account.

Fig. 5 shows the calculated results for T_{max} and T_{min} as a function of curve radius. The reference value for the radius is 400 m. Buckling starts at lower temperatures in small-radius curves.

The ballast behaviour, represented by the lateral peak and limit resistance, was varied over a range of 50-150% of the reference value. Fig. 6 shows T_{max} to be more sensitive to this factor. Fig. 7 indicates that varying the longitudinal ballast stiffness has little influence on T_{max}.

The torsional stiffness, often associated with the frame stiffness of the track, influences neither T_{max} nor T_{min}, as can be seen from Fig. 8.

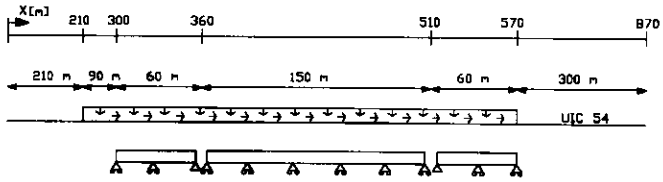

Fig. 11: Track model of fly-over

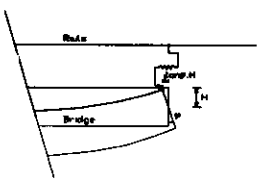

Fig. 12: Modelling the influence of bridge-end rotation

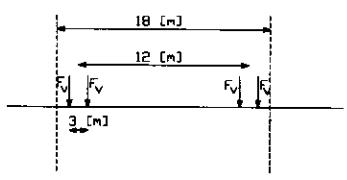

Fig. 13: Loading of the track

From Fig. 9, it is apparent that the amplitude of the misalignment has a marked influence on T_{max}, whereas T_{min} is less affected. The half wavelength, shown in Fig. 10, is related to the amplitude of the misalignment. In the calculations, a fixed relationship was assumed, based on statistical analysis of measurement data.

Longitudinal forces in the NS fly-over at Maartensdijk

Figs. 11-13 show how CWERRI was used to model a fly-over constructed for Netherlands Railways (NS) at Maartensdijk. The longitudinal ballast springs between rail and bridge were modelled as indicated in Fig. 12, and were connected in the middle of the sleeper and on top of the bridge deck. The model was loaded in four steps:

— a thermal load consisting of a temperature increase of 40°C for the rails and 20°C for the bridge;
— 20 wagons loading the track with a total of 80 axles, according to Figs. 11 and 13, each axle generating 225 kN vertically and 45 kN longitudinally. The longitudinal ballast strength was 20 kN per metre of unloaded track and 50 kN for loaded;
— in the third load step the track was unloaded from the longitudinal and vertical axle loads;
— finally, rail and bridge were thermally unloaded, which resulted in residual deformations and forces due to yielding of the ballast.

Results: some results are presented here by way of example, in order to illustrate the potential of the program. Fig. 14 shows the longitudinal forces in the rails. The relative longitudinal displacements between rails and bridge, an important measure of ballast degradation, are shown in Fig. 15.

Obviously, the thermal load step results in an asymmetric response, because both construction and load are asymmetric. Unloading in the fourth load step resulted in residual forces and displacements. The largest residual values in rail and ballast were obtained at both ends of each of the three bridge spans, where most of the ballast yield took place.

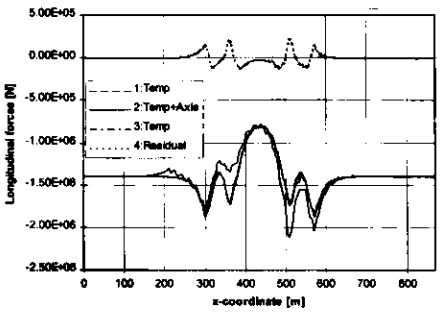

Fig. 14: Longitudinal forces in the rail

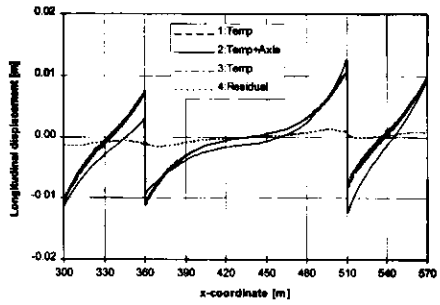

Fig. 15: Relative rail-bridge displacement

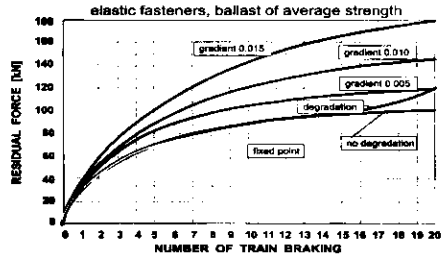

Fig. 17: Examples of creep calculations

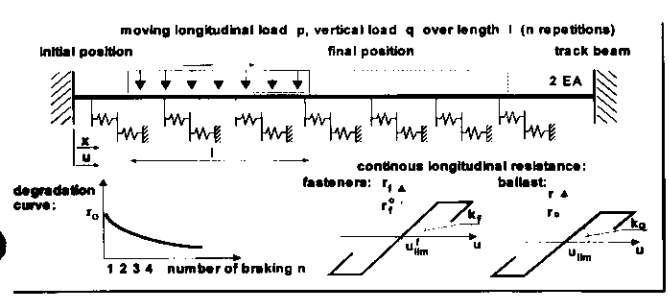

Fig. 16: CREEP model

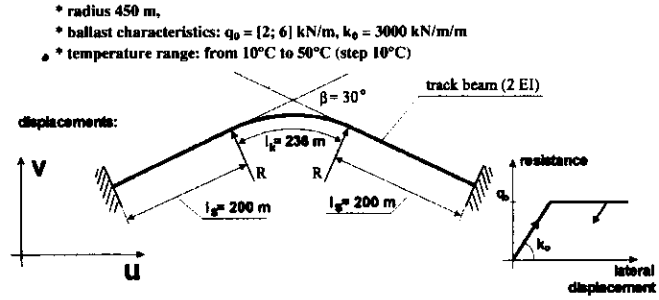

Fig. 18: Model applied for analysis of creep in sharp curves

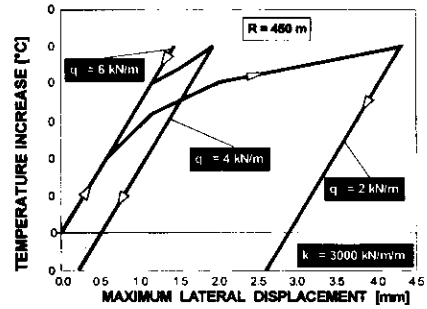

Fig. 19: Lateral movements of sharp curves

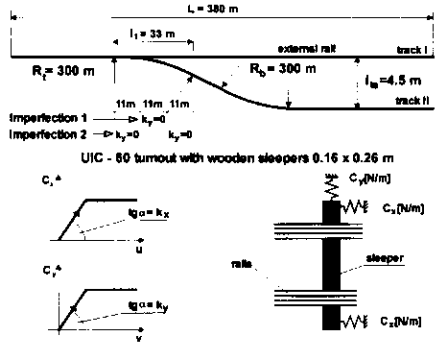

Fig. 20: Turnout model

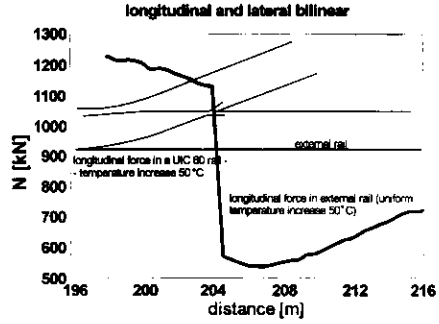

Fig. 21: Results of turnout analysis; longitudinal force in external stock rail

CREEP – longitudinal creep analysis

In the following paragraphs work carried out at the Technical University of Kraków, Poland, with respect to the analysis of longitudinal creep is discussed, and the CREEP model, which has been specially designed for this purpose, presented. The scope of the CREEP model is outlined in Fig. 16. The load is considered as a quasi-static moving load. The effect of the change in longitudinal resistance under vertical load is included. Ballast and fastener resistance are modelled bi-linearly, as also indicated in Fig. 16. Further, it is assumed that the ballast deteriorates with the increase in the number of brake applications according to a decaying exponential function of the form:

$$r^* = r_0 1.0306e^{-0.03n}$$

where: r_0 = yield point of the ballast without degradation and n = the number of loading passes. The sensitivity to ballast and fastener characteristics was investigated in [4]. The parameters were varied around the following mean values: r^0_f = 8.0 kN/m, k_f = 5,700 kN/m/m for the fasteners; and r_0 = 12.0 kN/m, k_0 = 8,000 kN/m/m for the ballast. The type of load was chosen in accordance with the data published in ERRI D 192/RP [5], i.e. vertical q = 86.25 kN/m; length of the load l = 640 m (DB, heavy); longitudinal braking load is p = hq [kN/m], with h = 0.2. Three gradients were considered: 5‰, 10‰ and 15‰. The influence of each gradient was taken into account as an increase in the braking force by the product of the value of the gradient and the braking load. In addition, fixed points were introduced to model a turnout with a length of 33 m and a longitudinal stiffness of 100 MN/m/m. The turnout was located 10 m ahead of the point where the train stopped.

Fig. 17 summarises the residual forces versus the number of brake applications. The influence of the gradient is quite significant, as is the effect of ballast degradation.

Sharp curves

The CREEP model also allows analysis of the lateral breathing of curves. As an example, the curve represented in Fig. 18 was studied with the different values of ballast resistance parameters of Fig. 16. The results, presented in Fig. 19, show how important a role ballast properties play.

TURN – turnout analysis

The model developed for analysing turnouts – TURN – is based on the finite element package ALGOR. This model, represented in Fig. 20, consists of a standard 1:9 turnout, comprised of UIC 60 rails, with a radius of curvature for the diverging track of 300 m. The timber sleepers have a cross section of 0.16 m x 0.26 m. A temperature increase of ΔT = 50°C was applied (equivalent rail force of 922 kN).

Fig. 21 illustrates the results of a calculation in which both the longitudinal and the lateral ballast resistance were modelled bi-linearly, with k_x = 1,500 kN/m/m, c_x^{lim} = 4.5 kN and u_{lim} = 3 mm for the longitudinal resistance; and k_y = 2,000 kN/m/m, c_y^{lim} = 9 kN and v_{lim} = 4.5 mm for the lateral resistance. Fig. 21 also shows that the longitudinal force increases by about 30% relative to the CWR force in the undisturbed state.

CWR safety fundamentals/philosophy

The basic premise for CWR buckling safety assurance lies in the performance-based requirement that CWR track should have the buckling strength required to withstand the environmentally and operationally imposed loads for the range of expected operating conditions. The translation of this statement into viable and *usable* safety specifications requires a rational CWR buckling safety management methodology [6]. This methodology consists of the application of the following four key elements:

— CWR track system/component characterisation;
— conduct buckling/stability analyses;
— establish and apply safety criteria;
— perform safety evaluation;

which requires the application of a dynamic or quasi-dynamic buckling analysis/model, such as for instance the U.S. Department of Transportation (DOT) CWR-BUCKLE program [7] or the CWERRI model. With respect to safety evaluation, this requires either the application of the safety criteria to directly perform a buckling safety evaluation and determine reserve buckling strength, or to develop safety guidelines/specifications in terms of allowable temperature increase limits as functions of track parameters/conditions, and apply these specifications for safety assessments.

Safety concepts and criteria

Buckling safety assurance should start with adopting an allowable, or permissible, temperature increase, T_{ALL}, *which should be larger than the anticipated maximum rail temperature increase in relation to the neutral temperature, i.e.:*

$$T_{ALL} > (T_R - T_N)$$

T_R = maximum rail temperature
T_N = neutral rail temperature

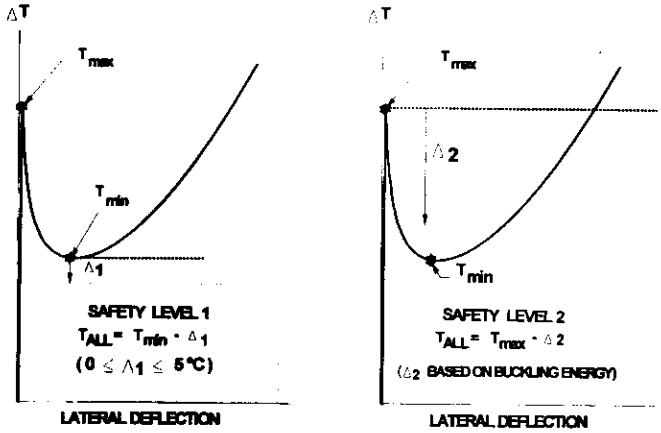

Fig. 22: Safety criterion definition in terms of allowable temperature increase for safety levels 1 and 2

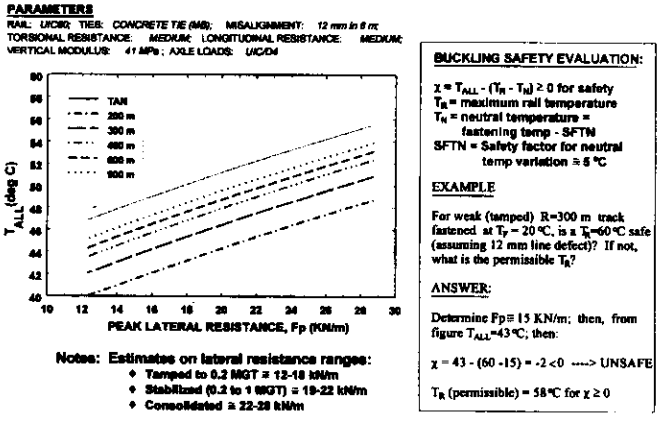

Fig. 23: Buckling safety limits for CWR tracks, based on safety level 1 with $\Delta_1 = 0$

T_{ALL} can be considered as the required buckling strength which is dependent on the governing track and vehicle parameters discussed above. T_{ALL} can be derived by applying an appropriate stability criterion to the analytically determined buckling response curves, or it can be empirically determined by dynamic buckling tests.

Buckling response curves, illustrated in Fig. 22, provide the basis for the allowable temperature T_{ALL}. These equilibrium curves are characterised by an upper and lower temperature. Buckling can take place in between these two temperatures. The allowable temperature can be based on either the *lower critical temperature*, T_{min}, minus a safety margin or the *upper critical temperature*, T_{max}, minus a safety margin depending on the levels of safety desired:

$$\text{Safety Level 1: } T_{ALL} = T_{min} - \Delta_1$$
$$\text{Safety Level 2: } T_{ALL} = T_{max} - \Delta_2$$

In this definition, Level 1 is more conservative, i.e. safer than Level 2; and Δ_1 and Δ_2 are safety margins associated with Levels 1 and 2. Using the lower critical temperature, T_{min}, as a baseline for allowable temperature is based on the fact that it guarantees, although not absolutely, the safety of CWR track against buckling since only above this temperature exist possible buckled configurations. Research has shown that at this lower critical temperature the energy of buckling is high, hence the T_{ALL} is fairly conservative.

Fig. 23 provides an example of safety limits in terms of T_{ALL} versus lateral resistance for a typical European track structure. In these calculations a range of track curvatures and lateral resistance values have been considered. T_{ALL} has been computed using Safety Level 1, with $\Delta_1 = 0$. It is obvious that with this conservative criterion, based on T_{min}, relatively low T_{ALL} values are found.

The D 202 Committee is presently working on a more suitable criterion to be incorporated in UIC leaflet 720 [8]. Broadly speaking, first a longitudinal force distribution has to be calculated with the aid of CWERRI, followed by an increase of the temperature until the track becomes unstable. This criterion should be based on both T_{min} and T_{max}.

Conclusions

The work of the ERRI D 202 Specialists' Committee has resulted in the development of versatile and user-friendly track analysis programs. These programs are now being used by the Committee to draft proposals for the revision of the UIC leaflets concerning CWR [8], [9]. One of the objectives is to look in more detail at the safety concepts for CWR track; CWERRI is one of the tools vital to the achievement of these objectives. The whole D 202 project is envisaged to be completed by the end of 1997.

References

[1] Esveld C.: 'How safe is CWR?', paper presented at the WCRR'96 – World Conference on Railway Research, Colorado Springs, Colorado, USA, 17-19 June 1996.

[2] Van M.A., Dieterman H.A.: 'Sensitivity analysis of buckling of curved CWR-track and a Fly-over study', TU Delft, Rp. 3.21.1.22.33, November 1995.

[3] Samavedam G., Kish A., Purple A., Schoengart J.: 'Parametric Analysis and Safety Concepts of CWR Buckling', US DOT-VNTSC-FRA-93-25, Washington, D.C., USA, December 1993.

[4] Czyczula W., Solkowski J.: 'Longitudinal track movement and sharp curves', TU Kraków, Poland, October 1995.

[5] ERRI D 202, RP 1: 'Proposal for theoretical model investigations concerning CWR', August 1994.

[6] Kish A., Samavedam G.: 'Dynamic buckling of continuous welded rail track: theory, tests and safety concepts', Transportation Research Record N01289, U.S. Department of Transportation, Washington, D.C., USA, Conference on 'Lateral Track Stability', 1991.

[7] Kish A., Samavedam G.: 'CWR-BUCKLE', Version 1.06 (1994) and User's Guide and Version 2 (1996), U.S. Department of Transportation, Washington, D.C., USA.

[8] UIC Leaflet 720 R: 'Laying and maintenance of track made up of continuous welded rails – 7th draft of 2nd edition', Paris, France, 1994.

[9] UIC Leaflet 774-3: 'Track/Bridge interaction', Paris, France, February 1995.